

Liquid phase separation controlled by pH

Omar Adame-Arana,¹ Christoph A. Weber,^{1,2} Vasily Zaburdaev,^{3,4} Jacques Prost,^{5,6} and Frank Jülicher^{1,2,7}

¹*Max-Planck-Institut für Physik komplexer Systeme,
Nöthnitzer Str. 38, 01187 Dresden, Germany*

²*Center for Systems Biology Dresden,
Pfortenhauerstr. 108, 01307 Dresden, Germany*

³*Friedrich-Alexander Universität Erlangen-Nürnberg,
Cauerstr. 11, 91058 Erlangen, Germany*

⁴*Max-Planck-Zentrum für Physik und Medizin,
Staudtstr. 2, 91058 Erlangen, Germany*

⁵*Laboratoire Physico Chimie Curie,
Institut Curie, PSL Research University,
CNRS UMR168, 75005 Paris, France*

⁶*Mechanobiology Institute, National University of Singapore,
5A Engineering Drive 1, Singapore 117411, Singapore*

⁷*Cluster of Excellence Physics of Life,
Technische Universität Dresden, 01062 Dresden, Germany*

(Dated: October 16, 2019)

Abstract

We present a minimal model to study liquid phase separation in a fixed pH ensemble. The model describes a mixture composed of macromolecules that exist in three different charge states and have a tendency to phase separate. We introduce the pH dependence of phase separation by means of a set of reactions describing the protonation and deprotonation of macromolecules, as well as the self-ionisation of water. We use conservation laws to identify the conjugate thermodynamic variables at chemical equilibrium. Using this thermodynamic conjugate variables we perform a Legendre transform which defines the corresponding free energy at fixed pH. We first study the possible phase diagram topologies at the isoelectric point of the macromolecules. We then show how the phase behavior depends on pH by moving away from the isoelectric point. We find that phase diagrams as a function of pH strongly depend on whether oppositely charged macromolecules or neutral macromolecules have a stronger tendency to phase separate. We predict the existence of reentrant behavior as a function of pH. In addition, our model also predicts that the region of phase separation is typically broader at the isoelectric point. This model could account for both, the protein separation observed in yeast cells for pH values close to the isoelectric point of many cytosolic proteins and also for the *in vitro* experiments of single proteins exhibiting phase separation as a function of pH.

I. INTRODUCTION

One of the central challenges in biology is to understand the spatial organisation of cells. Cells are organised in distinct compartments which provide specific biochemical environments that play a role for many physico-chemical processes such as the production of ATP or the assembly of cellular building blocks [1]. In many cases the cell achieves spatial organisation of its biochemistry by forming membrane-less organelles, such as P granules, stress granules and centrosomes [2–4]. It has been shown in recent years that many membrane-less organelles have liquid like properties. They are condensates of certain types of protein and often RNA that can be best understood as forming by a phase separation process [2, 5–8].

While some of these compartments persist for longer times, others, such as stress granules form rapidly in response to stimulus such as changes in temperature, pH or depletion of nutrients [9]. The formation of liquid-like condensates can also be reconstituted *in vitro* using purified proteins [10, 11].

The formation of protein condensates is also important in other contexts. The cytoplasm of yeast cells was shown to transition from a fluid-like to an arrested solid-like state during nutrient depletion [12]. This transition is reversible and provides a protective mechanism that helps cells to survive periods of nutrient depletion until conditions improve and nutrients become available again. The biophysical mechanism responsible for this transition has been linked to changes in the cytosolic pH. The effects of pH on yeast cells can be described as follows. During nutrient depletion, a yeast cell does not have sufficient resources to supply proton pumps that are responsible for regulating the intracellular pH. As a result, in an acidic environment, natural for yeast habitat, the pH of the cytoplasm drops and many cytosolic proteins become insoluble. If the resulting protein condensates occupy a large volume fraction of the cytoplasm, the cytoplasm can transition from a fluid-like to a solid-like arrested state. This observation suggests that the reduction of pH triggers phase separation of proteins from solution. Interestingly, in this case, phase separation is triggered as the pH of the solution moves closer to the isoelectric points of many cytosolic proteins. This raises the question why pH changes, and in particular, pH values in the vicinity of the isoelectric point, promote phase separation. More generally we want to understand how the formation of protein condensates can be regulated by changes in pH.

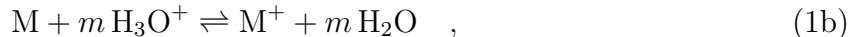
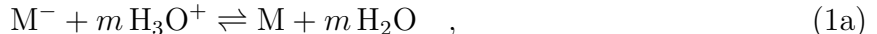
To address this question we present a generic thermodynamic framework to study the influence of pH on liquid-liquid phase separation. The key idea is to couple a system capable of undergoing phase separation with a set of chemical reactions corresponding to the protonation/deprotonation of water components and macromolecules such as proteins. We consider two types of interactions, namely attractive interactions between oppositely charged macromolecules in the presence of counterions and salt, and attractive interactions among neutral macromolecules that could be mediated for example by Van der Waals or hydrophobic interactions. Using conservation laws and chemical equilibrium conditions [13], we construct an effective thermodynamic potential describing a system with pH as a thermodynamic variable. We then use this thermodynamic potential to determine the phase behaviour of the system as a function of the molecular properties and pH. We find coexisting phases of different compositions of charged and uncharged macromolecules. We show that the compositions of the coexisting phases can be controlled by changing pH.

The manuscript is organised as follows. In Section II, we introduce a set of chemical reactions in which the charge state of a macromolecule is fixed by the pH of the system. We then define the pH and show its relation to the previously introduced chemical reactions.

In Section III we present the thermodynamics of multicomponent mixtures and discuss the parameter choices for our study. We study the thermodynamic equilibrium for a system with fixed pH in Section IV, whereby using conservation laws we identify the thermodynamic conjugate variables of the system which we then use to construct the corresponding thermodynamic potential for fixed pH. In Section V, we introduce new composition variables and thermodynamic fields controlling phase separation and discuss chemical and phase equilibrium in terms of the newly defined variables. In Sections VI and VII, we study the phase behaviour at and away from the isoelectric point respectively. Finally, we discuss our results in Section VIII.

II. CHEMICAL REACTIONS AND PH IN MACROMOLECULAR SYSTEMS

We study a multicomponent mixture of macromolecules which can exist in three different charge states. Macromolecules with a maximal positive net charge $+m$ are denoted by M^+ , those with maximal negative net charge $-m$ by M^- and neutral macromolecules are denoted by M . We also consider water molecules H_2O , hydronium ions H_3O^+ and hydroxide ions OH^- . We describe both protonation and deprotonation of the macromolecules as well as the self-ionisation of water with the following chemical reactions



The average charge state of the macromolecules determined from reactions (1) is controlled by the pH of the mixture. The pH is defined as [14]

$$\text{pH} = -\log_{10} a_{H^+} \quad , \quad (2)$$

with the relative activity of the proton a_{H^+} given by

$$a_{H^+} = \exp\left(\frac{\mu_{H^+} - \mu_{H^+}^0}{k_B T}\right) \quad , \quad (3)$$

where k_B is the Boltzmann constant, μ_{H^+} is the chemical potential of protons in the system and $\mu_{H^+}^0$ denotes the chemical potential of protons in a reference state [15]. The definition of pH in Eq. (2) refers to the proton activity. Protons in water are typically hydrated [16, 17]. At chemical equilibrium, the proton hydration reaction $H^+ + H_2O \rightleftharpoons H_3O^+$, implies the relation $\mu_{H^+} = \mu_{H_3O^+} - \mu_{H_2O}$, where $\mu_{H_3O^+}$ is the chemical potential of the hydronium ions and μ_{H_2O} is the chemical potential of water. Therefore, the proton activity (Eq. (3)) can be written as

$$a_{H^+} = \exp\left(\frac{(\mu_{H_3O^+} - \mu_{H_2O}) - (\mu_{H_3O^+}^0 - \mu_{H_2O}^0)}{k_B T}\right) \quad , \quad (4)$$

where the reference chemical potentials, $\mu_{H_3O^+}^0$ and $\mu_{H_2O}^0$ define the pH scale. A standard choice for the reference chemical potentials are the chemical potential of the hydronium ions $\mu_{H_3O^+}^0$ at strong dilution evaluated at a standard concentration ($n_{H_3O^+}^0 = 1 \text{ M}$) and the chemical potential of pure water $\mu_{H_2O}^0$ [15]. In the strong dilution limit, the proton activity is $a_{H^+} \simeq n_{H_3O^+}/n_{H_3O^+}^0$, leading to $\text{pH} \simeq -\log_{10} n_{H_3O^+}$, where $n_{H_3O^+}$ denotes the concentration of the H_3O^+ ions (see the Supplementary Material). In this paper we use Eqs. (2) and (4) to define the pH. Next, we describe a thermodynamic framework to quantify the effect of pH on phase separation behaviour in this macromolecular system.

III. THERMODYNAMICS OF MULTICOMPONENT MIXTURES

We consider an incompressible multicomponent mixture in the (T, P, N_i) ensemble with temperature T , pressure P and N_i denoting the number of particles of component i in the mixture. The corresponding thermodynamic potential is the Gibbs free energy $G(T, P, N_i)$. The chemical potential is defined by $\mu_i = \partial G / \partial N_i|_{T, P, N_j \neq i}$, the entropy is $S = -\partial G / \partial T|_{P, N_i}$ and the volume of the system is $V = \partial G / \partial P|_{T, N_i}$. By incompressibility we mean that the molecular volumes of each component, $v_i = \partial V / \partial N_i|_{T, P, N_j \neq i}$ are independent of pressure and composition. The volume density of the Gibbs free energy is given by $g(T, P, n_i) = G(T, P, N_i) / V(N_i)$, where we have introduced the concentrations $n_i = N_i / V$ and the volume $V(N_i) = \sum_i v_i N_i$. The chemical potentials can then be calculated from the Gibbs free energy density by

$$\mu_i = v_i \left(g - \sum_k \frac{\partial g}{\partial n_k} n_k \right) + \frac{\partial g}{\partial n_i} . \quad (5)$$

We study the multicomponent mixture using a Flory-Huggins mean field free energy model where the Gibbs free energy density reads [18, 19]:

$$g = k_B T \sum_k n_k \ln(n_k v_k) + \sum_k w_k n_k + \sum_{kl} \frac{\Lambda_{kl}}{2} n_k n_l + P . \quad (6)$$

The logarithmic terms stem from the mixing entropy, w_k denote internal free energies of molecules of type k and the interaction parameters Λ_{kl} describe the contribution to the free energy due to molecular interactions. Molecular interactions can outcompete the mixing entropy and cause the emergence of coexisting phases. Using the free energy density Eq. (6), the chemical potentials are

$$\mu_i = v_i(P - \Sigma) + w_i + k_B T (\ln(n_i v_i) + 1) + \sum_k \Lambda_{ik} n_k , \quad (7)$$

where Σ is defined by

$$\Sigma = \sum_{kl} \frac{\Lambda_{kl}}{2} n_k n_l + k_B T \sum_k n_k . \quad (8)$$

In the multicomponent mixture we consider, the indices i, k and l run over the six components of the system, which are the three charge states of the macromolecules M, M^+, M^- as well as the three charge states of water H_2O, H_3O^+ and OH^- . We further consider the molecular volumes of the macromolecules to be all equal, $v = v_M = v_{M^+} = v_{M^-}$, where we have introduced the macromolecular volume v . We also consider the molecular volumes of water and water ions to be the same, $v_0 = v_{H_2O} = v_{H_3O^+} = v_{OH^-}$, and denote them by v_0 . In order to have a minimal number of components, the presence of salt and counterions which neutralise our solution are taken into account implicitly. The presence of salt and counterions screen the electrostatic interactions, thus providing a characteristic length scale of the interaction potentials between charged species, while the counterions mediate the interactions between oppositely charged macromolecules, hence giving an effective interaction between them. The effective interactions in our system are captured by the interaction matrix Λ_{ij} . We consider all effective interactions $\Lambda_{ij} = 0$ except for those between positively and negatively charged macromolecules which we choose as $\Lambda_{M^-M^+} = \Lambda_{M^+M^-} = v\chi_e/\epsilon$ and the

effective interaction between neutral macromolecules given by $\Lambda_{\text{MM}} = 2v\chi_{\text{n}}/\epsilon$. Here we have introduced the molecular volumes ratio $\epsilon = v_0/v$ as well as χ_{e} and χ_{n} which are interaction parameters characterising the strength of charge-charge and neutral-neutral interactions respectively, with this choice, the interaction parameters describe the scale corresponding to a water molecule. Attractive interactions are described by negative values of these interaction parameters, which we will vary in our study of phase behaviour. In the following, we study the system at chemical equilibrium for a fixed pH.

IV. CHEMICAL EQUILIBRIUM AT FIXED PH

We start by stating the conservation laws for a system undergoing reactions (1) and identify the conserved quantities as independent composition variables at chemical equilibrium. We then use these independent composition variables to identify the thermodynamic conjugated variables at chemical equilibrium. We finalise the section by constructing a thermodynamic potential which describes the system at a fixed pH value.

A. Chemical conservation laws

We consider a system with s different molecular species. If there are r different chemical reactions taking place, there exist $c = s - r$ independent composition variables. Here $s = 6$, the number of independent reactions is $r = 3$, therefore the number of independent composition variables is $c = 3$. These independent composition variables can be chosen as conserved quantities during chemical reaction events. Although the number of independent composition variables is fixed, there is no unique choice of conserved variables [13]. We choose to use the total number of macromolecules in the system N , the amount of oxygen N_s and the net charge involved in the chemical reactions N_q (see the Supplementary Material), given as:

$$N = N_{\text{M}^-} + N_{\text{M}} + N_{\text{M}^+} \quad , \quad (9\text{a})$$

$$N_s = N_{\text{H}_3\text{O}^+} + N_{\text{OH}^-} + N_{\text{H}_2\text{O}} \quad , \quad (9\text{b})$$

$$N_q = N_{\text{H}_3\text{O}^+} - N_{\text{OH}^-} + m(N_{\text{M}^+} - N_{\text{M}^-}) \quad . \quad (9\text{c})$$

Note that the net charge is neutralised by counterions that are not explicitly considered in the simplified model.

B. Conjugate thermodynamic variables at chemical equilibrium

We obtain conditions for chemical equilibrium in terms of the conserved variables defined in Eqs. (9), and to do so, we use the variable transformation $(N_{\text{M}}, N_{\text{H}_3\text{O}^+}, N_{\text{H}_2\text{O}}) \rightarrow (N, N_s, N_q)$ to eliminate $N_{\text{M}}, N_{\text{H}_3\text{O}^+}$ and $N_{\text{H}_2\text{O}}$. The differential of the Gibbs free energy is

given by $dG = -SdT + VdP + \sum_i \mu_i dN_i$, which after this variable transformation becomes:

$$\begin{aligned}
dG = & -S dT + V dP + \mu_M dN + \mu_{H_2O} dN_s \\
& + (\mu_{H_3O^+} - \mu_{H_2O}) dN_q \\
& + (\mu_{M^-} + m \mu_{H_3O^+} - \mu_M - m \mu_{H_2O}) dN_{M^-} \\
& + (\mu_{M^+} + m \mu_{H_2O} - \mu_M - m \mu_{H_3O^+}) dN_{M^+} \\
& + (\mu_{H_3O^+} + \mu_{OH^-} - 2\mu_{H_2O}) dN_{OH^-} \quad .
\end{aligned} \tag{10}$$

If the system has reached chemical equilibrium, the variations dG with respect to changes in the non-conserved composition variables N_{M^+} , N_{M^-} and N_{OH^-} must vanish. This then leads to the following chemical equilibrium conditions [20]:

$$\mu_{M^-} + m \mu_{H_3O^+} = \mu_M + m \mu_{H_2O} \quad , \tag{11a}$$

$$\mu_M + m \mu_{H_3O^+} = \mu_{M^+} + m \mu_{H_2O} \quad , \tag{11b}$$

$$\mu_{H_3O^+} + \mu_{OH^-} = 2 \mu_{H_2O} \quad . \tag{11c}$$

Using the chemical equilibrium conditions, the differential of the Gibbs free energy at chemical equilibrium is therefore

$$\begin{aligned}
dG = & -S dT + V dP + \mu_M dN + \mu_{H_2O} dN_s \\
& + (\mu_{H_3O^+} - \mu_{H_2O}) dN_q \quad ,
\end{aligned} \tag{12}$$

which explicitly shows that the Gibbs free energy at chemical equilibrium has the dependence $G(T, P, N, N_s, N_q)$. This allows us to identify pairs of conjugate thermodynamic variables. From Eq. (12) we identify the conjugate thermodynamic variables to the composition variables (N, N_s, N_q) as $(\mu_M, \mu_{H_2O}, \mu_{H_3O^+} - \mu_{H_2O})$ respectively. These conjugate variables have to be used to obtain Legendre transforms of the thermodynamic potentials [13].

C. Thermodynamic ensemble for fixed pH

In order to describe the system in an ensemble with pH as a variable, we perform a Legendre transform to construct a thermodynamic potential which depends on $\mu_{H_3O^+} - \mu_{H_2O}$. This thermodynamic potential is given by the following Legendre transform

$$\bar{G}(T, P, N, N_s, \mu_{H_3O^+} - \mu_{H_2O}) = G - (\mu_{H_3O^+} - \mu_{H_2O}) N_q \quad . \tag{13}$$

The differential of \bar{G} reads

$$\begin{aligned}
d\bar{G} = & -S dT + V dP + \mu_M dN + \mu_{H_2O} dN_s \\
& - N_q d(\mu_{H_3O^+} - \mu_{H_2O}) \quad .
\end{aligned} \tag{14}$$

We now clarify why fixing this chemical potential difference and the temperature sets the pH value of the system. Using Eq. (2) and Eq. (4), we can express the pH as

$$\text{pH} = \frac{(\mu_{H_3O^+} - \mu_{H_2O}) - (\mu_{H_3O^+}^0 - \mu_{H_2O}^0)}{k_B T} \log_{10} e \quad , \tag{15}$$

where it is explicitly shown that the pH of the system is set by the relative chemical potential of hydronium ions with respect to water, $\mu_{\text{H}_3\text{O}^+} - \mu_{\text{H}_2\text{O}}$, and the temperature T of the system. We can also define the corresponding free energy in the isochoric ensemble as

$$\bar{F} = G - (\mu_{\text{H}_3\text{O}^+} - \mu_{\text{H}_2\text{O}})N_q - PV \quad , \quad (16)$$

which has the following differential form

$$\begin{aligned} d\bar{F} = & -SdT - PdV + \mu_M dN + \mu_{\text{H}_2\text{O}} dN_s \\ & - N_q d(\mu_{\text{H}_3\text{O}^+} - \mu_{\text{H}_2\text{O}}) \quad . \end{aligned} \quad (17)$$

In our system, the volume V can be expressed in terms of the conserved quantities as $V = vN + v_0N_s$, leading to $dN_s = dV/v_0 - vdN/v_0$. We can then reduce the number of independent variables and rewrite the differential form of \bar{F} as

$$d\bar{F} = -S dT - \Pi dV + \bar{\mu}_M dN - N_q d\bar{\mu}_{\text{H}_3\text{O}^+} \quad , \quad (18)$$

where we have introduced the exchange chemical potentials $\bar{\mu}_M$ of neutral macromolecules and $\bar{\mu}_{\text{H}_3\text{O}^+}$ of hydronium ions as well as the osmotic pressure Π , which are defined by

$$\bar{\mu}_i = \mu_i - \frac{v_i}{v_0} \mu_{\text{H}_2\text{O}} \quad , \quad (19)$$

$$\Pi = P - \frac{\mu_{\text{H}_2\text{O}}}{v_0} \quad , \quad (20)$$

where $i = M$ or H_3O^+ . The free energy $\bar{F}(T, V, N, \bar{\mu}_{\text{H}_3\text{O}^+})$ depends only on the temperature T , the volume V , the total macromolecule particle number N and the exchange chemical potential of the hydrogen ions $\bar{\mu}_{\text{H}_3\text{O}^+}$. In addition to introducing the corresponding thermodynamic potential \bar{F} which describes an incompressible system with a fixed pH value, we have reduced our multicomponent system description from six components undergoing three independent chemical reactions to an effective binary mixture with the total macromolecule density $n = N/V$ as the only relevant composition variable. We can now ask how the pH affects phase separation.

V. CONTROL OF PHASE SEPARATION BY PH

In the following, we discuss how the pH controls both, chemical and phase equilibrium in our system. We start by discussing the chemical equilibrium conditions (11) in terms of newly defined composition variables and thermodynamic field. After discussing the chemical equilibrium conditions in terms of the pH and the newly defined fields, we provide the conditions for phase equilibrium for a system described by the corresponding thermodynamic potential defined by (16). We end the section by showing a construction of the coexisting phases for a given choice of parameters.

A. Thermodynamic fields controlling chemical equilibrium

We are now interested in discussing how the pH and other parameters influence the chemical equilibrium described by conditions (11). In order to do so, we introduce thermodynamic

fields and composition variables which allow us to interpret the chemical equilibrium conditions intuitively. Let us first introduce the following composition variables

$$n = n_{M^+} + n_{M^-} + n_M \quad , \quad (21)$$

$$\phi = \frac{n_{M^+} + n_{M^-}}{2n} \quad , \quad (22)$$

$$\psi = \frac{n_{M^+} - n_{M^-}}{2n} \quad . \quad (23)$$

These composition variables express the total concentration of macromolecules n , the fraction of charged macromolecules ϕ and the difference between concentrations of oppositely charged macromolecules relative to the total number of macromolecules ψ .

It is convenient to make a rearrangement of the chemical equilibrium conditions (11) as follows

$$\mu_{M^+} + \mu_{M^-} = 2\mu_M \quad , \quad (24a)$$

$$\mu_{M^+} - \mu_{M^-} = 2m(\mu_{H_3O^+} - \mu_{H_2O}) \quad , \quad (24b)$$

$$\mu_{H_2O} - \mu_{OH^-} = \mu_{H_3O^+} - \mu_{H_2O} \quad , \quad (24c)$$

where we see that the right hand sides of Eqs. (24b) and (24c) are determined by the pH. We now write the conditions (24a) and (24b) in terms of the composition variables using the expressions of the chemical potentials (Eqs. (S.6)) leading to

$$k_B T \ln \frac{\phi^2 - \psi^2}{(1 - 2\phi)^2} + \frac{2v\chi_e n \phi}{\epsilon} - \frac{4v\chi_n n(1 - 2\phi)}{\epsilon} = h_\phi \quad , \quad (25)$$

$$k_B T \ln \frac{\phi + \psi}{\phi - \psi} - \frac{2v\chi_e n \psi}{\epsilon} = h_\psi \quad , \quad (26)$$

where we have defined

$$h_\phi = 2w_M - w_{M^+} - w_{M^-} \quad , \quad (27)$$

$$h_\psi = 2m(\mu_{H_3O^+} - \mu_{H_2O}) - w_{M^+} + w_{M^-} \quad . \quad (28)$$

These quantities play the role of fields controlling the chemical equilibrium and phase separation behaviour of the system. The molecular field h_ϕ characterises which of the macromolecular charge states is energetically favoured due to their internal free energies w_i , while the field h_ψ expresses deviations of the pH from its value at the isoelectric point (pI) of the macromolecules. Remember that the isoelectric point is the value of the pH for which macromolecules are on average neutral. Thus, in our system, the isoelectric point is defined as the value pI of the pH at which the charged macromolecules obey, $n_{M^+} = n_{M^-}$, or equivalently $\psi = 0$, which implies $h_\psi = 0$ via Eq. (26). Using Eq. (15), we find an expression for the pI value:

$$\text{pI} = \left(\frac{w_{M^+} - w_{M^-}}{2mk_B T} - \frac{\mu_{H_3O^+}^0 - \mu_{H_2O}^0}{k_B T} \right) \log_{10} e \quad . \quad (29)$$

We can therefore express the field h_ψ in terms of the pH and the pI as follows

$$\frac{h_\psi}{k_B T} = \frac{2m}{\log_{10} e} (\text{pI} - \text{pH}) \quad , \quad (30)$$

which explicitly shows how h_ψ characterises deviations of the system from its isoelectric point. For given h_ϕ and h_ψ , the composition variables ϕ and ψ can be determined from Eqs. (25)-(26) as a function of the total macromolecule density n , the temperature T and the pH. One symmetry can be identified in Eqs. (24a) and (24b), namely that the system behaves identically under the transformation $\psi \rightarrow -\psi$ and $h_\psi \rightarrow -h_\psi$, which will be reflected in the phase diagrams as a function of deviations from the isoelectric point. This symmetry stems from both, considering that positively and negatively charged macromolecules have the same interaction with the rest of the components as well as from choosing their molecular volumes to be the same. Changing any of the two previously mentioned conditions would break this symmetry. We must note that in a more realistic scenario there would be differences in solvation of the two different charged states of the macromolecule [21].

We find the concentrations of water components by using the chemical equilibrium condition corresponding to the self-ionisation of water reaction and Eqs. (S.6e)-(S.6f). We then express the concentrations $n_{\text{H}_3\text{O}^+}$, n_{OH^-} and $n_{\text{H}_2\text{O}}$ in terms of two new fields h_H and h_O which only depend on the molecular properties of the water components and the pH of the system (the definitions of these fields as well as explicit formulas for the concentration of water components are provided in the Supplementary Material).

We have shown that chemical equilibrium can be fully accounted for by the internal free energies of all species w_i which we take to be constant, the temperature T , the pH (or equivalently the chemical potential difference $\mu_{\text{H}_3\text{O}^+} - \mu_{\text{H}_2\text{O}}$) and the total macromolecule concentration n .

B. Phase coexistence in the pH ensemble

We are interested in describing the phase behaviour of the system in the pH ensemble. To this end we make use of the composition variables n , ϕ and ψ and the fields h_ϕ , h_ψ , h_H and h_O defined in the previous section. Using Eq. (16) we define the free energy density $\bar{f}(T, n, \bar{\mu}_{\text{H}_3\text{O}^+}) = \bar{F}(T, V, N, \bar{\mu}_{\text{H}_3\text{O}^+})/V$ which reads

$$\begin{aligned} \bar{f}(T, n, \bar{\mu}_{\text{H}_3\text{O}^+}) = & k_{\text{B}}T \left[n(\phi + \psi) \ln(vn(\phi + \psi)) + n(\phi - \psi) \ln(vn(\phi - \psi)) \right. \\ & + n(1 - 2\phi) \ln(vn(1 - 2\phi)) \\ & + \frac{1}{v_0}(1 - vn) \ln \left(\frac{1 - vn}{1 + e^{h_H/k_{\text{B}}T + h_\psi/2mk_{\text{B}}T} + e^{h_O/k_{\text{B}}T - h_\psi/2mk_{\text{B}}T}} \right) \left. \right] \\ & + \frac{v}{\epsilon} \chi_e n^2 (\phi^2 - \psi^2) + \frac{v}{\epsilon} \chi_n n^2 (1 - 2\phi)^2 - h_\phi n \phi - h_\psi n \psi \\ & + w_{\text{M}} n + \frac{w_{\text{H}_2\text{O}}}{v_0} (1 - vn) \quad , \end{aligned} \quad (31)$$

where the functions $\phi(T, n, \bar{\mu}_{\text{H}_3\text{O}^+})$ and $\psi(T, n, \bar{\mu}_{\text{H}_3\text{O}^+})$ are defined implicitly in Eqs. (25) and (26) in terms of the temperature T , the exchange chemical potential of hydronium ions $\bar{\mu}_{\text{H}_3\text{O}^+}$ and the total macromolecule density n .

We now discuss the phase coexistence conditions for this incompressible system at fixed temperature T and at a fixed pH value, which can be obtained by a Maxwell construction. It follows from Eq. (18) that the exchange chemical potential of neutral macromolecules is given by $\bar{\mu}_{\text{M}} = \partial \bar{f} / \partial n|_{T, \bar{\mu}_{\text{H}_3\text{O}^+}}$ and that the osmotic pressure is given by $\Pi = \bar{f} - n \partial \bar{f} / \partial n|_{T, \bar{\mu}_{\text{H}_3\text{O}^+}}$. Using the free energy density \bar{f} , we write the phase equilibrium conditions describing equal

exchange chemical potentials of the neutral macromolecules and equal osmotic pressures in both phases [22]:

$$\bar{\mu}_M(n^I) = \bar{\mu}_M(n^{II}) \quad , \quad (32a)$$

$$\bar{\mu}_M(n^I) = \frac{\bar{f}(n^{II}) - \bar{f}(n^I)}{n^{II} - n^I} \quad , \quad (32b)$$

where the superscripts I, II denote the two coexisting phases. We did not write the explicit dependence of the relative chemical potential $\bar{\mu}_M$ and of the free energy density \bar{f} on the temperature T and on the relative chemical potential $\bar{\mu}_{\text{H}_3\text{O}^+}$. These conditions correspond to the common tangent construction [22]. We can find the coexisting phases by first calculating the values of ϕ and ψ using Eqs. (25) and (26) (Fig. 1(a,b)), and then by doing a common tangent construction for the free energy density Eq. (31) evaluated as a function of the total macromolecule volume fraction $\bar{n} = vn$ (Fig. 1(c)). The phase diagrams can then be readily constructed by repeating the steps described above for different parameter values.

VI. PHASE DIAGRAMS AT THE ISOELECTRIC POINT

In this section, we investigate different phase diagrams which can be obtained by varying temperature at constant total number of macromolecules, keeping the system at its isoelectric point. In order to discuss the effects of temperature we use a weighted sum of the interaction parameters $\chi = \chi_e + 4\chi_n$, the ratio of interaction parameters $\lambda = \frac{2\chi_n}{\chi_e + 4\chi_n}$, the molecular field h_ϕ and rewrite Eq. (25) and Eq. (31) in the following compact way:

$$h_\phi = 2k_B T \ln \frac{\phi}{(1-2\phi)} + \frac{2\chi\bar{n}(\phi-\lambda)}{\epsilon} \quad , \quad (33)$$

$$\begin{aligned} v\bar{f}(T, n, \bar{\mu}_{\text{H}_3\text{O}^+}) = k_B T & \left[2\bar{n}\phi \ln(\bar{n}\phi) + \bar{n}(1-2\phi) \ln(\bar{n}(1-2\phi)) \right. \\ & \left. + \frac{1}{\epsilon}(1-\bar{n}) \ln \left(\frac{1-\bar{n}}{1 + e^{h_{\text{H}}/k_B T} + e^{h_{\text{O}}/k_B T}} \right) \right] \\ & + \chi\epsilon^{-1}\bar{n}^2(\phi^2 - 2\lambda\phi + \lambda/2) - h_\phi\bar{n}\phi \\ & + \left(w_M - \frac{w_{\text{H}_2\text{O}}}{\epsilon} \right) \bar{n} + \frac{w_{\text{H}_2\text{O}}}{\epsilon} \quad . \end{aligned} \quad (34)$$

We further consider attractive interactions $\chi < 0$ and $\lambda > 0$. In order to construct phase diagrams as a function of temperature we rescale all the variables which have energy units with $k_B T_0$, where T_0 is a reference temperature. Free energy minimisation at constant $h_\phi, \chi, \lambda, \epsilon, h_{\text{H}}, h_{\text{O}}$ and T together with a common tangent construction, lead to different possible topologies of phase diagrams which are summarised in Fig. 2 and Fig. 3.

For $2\chi(1/2 - \lambda) > \epsilon h_\phi$, or $\epsilon h_\phi > -2\chi\lambda$, the diagram has the same topology as that of a simple two component mixture [23], see Fig. 2(a,d,e,h). At low temperature the system demixes in a low density and a high density phase. For $\epsilon h_\phi \ll 2\chi(1/2 - \lambda)$, the proportion of charged molecules is exponentially small and the system behaves like a neutral polymer solution. In this case the system separates into a low density phase and a high density phase composed essentially of neutral macromolecules $\phi \approx 0$. The coexistence curve is bell shaped and by construction the tie lines are parallel to the \bar{n} axis. The point at which the tangent is parallel to this axis is a critical point (Fig. 2(a,e)). It belongs to the same universality class

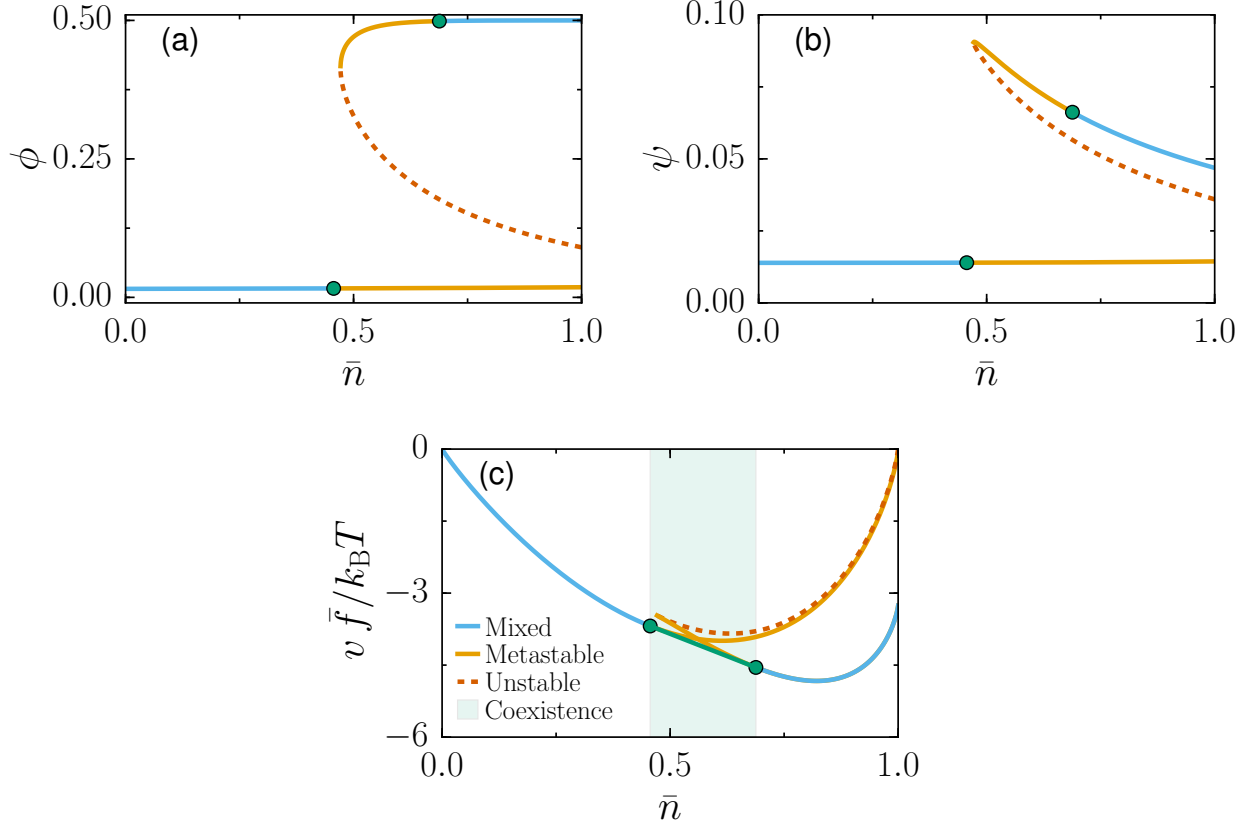


FIG. 1. Chemical equilibrium conditions and free energy density at chemical equilibrium. Multiple solutions are found for ϕ (a) and ψ (b) as a function of the total macromolecule volume fraction \bar{n} , enabling the system to exhibit phase separation between different branches of the chemical equilibrium. The blue solid lines correspond to equilibrium concentrations where the system remains homogeneous, the orange solid lines represent solutions to the chemical equilibrium relations which are metastable states and the dotted red line shows the unstable states. (c) Maxwell construction for the dimensionless free energy density $v\bar{f}/k_{\text{B}}T$ as a function of the total macromolecule volume fraction, the green line describes the region of macromolecule volume fraction where the system split into two phases with different compositions given by the green circles. Parameters $\chi_e/k_{\text{B}}T = -3$, $\chi_n = 0$, $p\text{I} - p\text{H} = 0.2$, $h_\phi/k_{\text{B}}T = -10$ and $\epsilon = 0.1$, apply to all panels.

as a liquid-vapour critical point. For $\epsilon h_\phi \gg -2\chi\lambda$, the concentration of neutral molecules is exponentially small and the system demixes between a low density phase and a high density phase composed essentially of charged molecules $\phi \approx 1/2$. Again the coexistence curve is "bell shaped" and one observes the existence of an isolated critical point (Fig. 2(d,h)).

In both limits, the mean-field calculation of the critical coordinates can be done analytically. The details are given in the Supplementary Material. In these limits, the critical

values are given by:

$$\bar{n}_c^b = \frac{\sqrt{\epsilon}}{1 + \sqrt{\epsilon}} \quad , \quad \text{for } \phi = 0 \text{ and } \phi = \frac{1}{2} \quad , \quad (35a)$$

$$kT_c^b = -\frac{2\chi_n}{(1 + \sqrt{\epsilon})^2} \quad , \quad \text{for } \phi = 0 \quad , \quad (35b)$$

$$kT_c^b = -\frac{\chi_e}{2(1 + \sqrt{\epsilon})^2} \quad , \quad \text{for } \phi = \frac{1}{2} \quad , \quad (35c)$$

where we have used the the condition for critical points, $\partial^2 \bar{f} / \partial n^2 = 0$ and $\partial^3 \bar{f} / \partial n^3 = 0$. We refer hereafter to these coexistence regions as quasi-binary regions.

For intermediate values of the molecular field, $2\chi(1/2 - \lambda) \lesssim \epsilon h_\phi \lesssim -2\chi\lambda$ the possible topologies of phase diagrams are more complex. Increasing the value of h_ϕ , from very large negative values towards positive values, leads to the emergence of a second coexistence region (Fig. 2(b,f)). This coexistence region, disconnected from the quasi-binary region, is bounded by a critical point and it is connected to the $\bar{n} = 1$ axis at a single point, where the tie line span vanishes. The transition point corresponds to a first order transition on the \bar{n} line, where ϕ undergoes a discontinuity. A second coexistence region emerges via a critical point, whose values are given by (Fig. 3(a,d)):

$$\phi_c = \frac{1}{4} \quad , \quad (36a)$$

$$kT_c = -\frac{\chi}{8\epsilon} \quad , \quad (36b)$$

$$h_{\phi,c} = \frac{\chi(2 + \ln(2) - 8\lambda)}{4\epsilon} \quad . \quad (36c)$$

The two phase region collapses to one point on the $\bar{n} = 1$ line, both in the first order and in the second order scenarios, this results from the existence of only one singularity in ϕ on the $\bar{n} = 1$ line. Note that $h_{\phi,c}$ can be either positive or negative, so that one can have a critical point on the $\bar{n} = 1$ line both in the neutral and in the charged regimes, see the Supplementary Material.

For some values of h_ϕ , with $h_\phi > h_{\phi,c}$, the two coexistence regions merge (Fig. 2(c,g)). Depending on λ , there may be two different generic scenarios. We first explain what happens for $\lambda < 1/4$. In this case, the two regions merge, giving rise to two triple points (Fig. 3(f)). The two triple points have a low density phase enriched in neutral macromolecules coexisting with both, an intermediate phase with a large macromolecule concentration, which is also rich in neutral macromolecules and with a macromolecule dense phase of essentially charged macromolecules. For $\epsilon h_\phi > 2\chi(1/4 - \lambda)$, one triple point and the first order transition point vanish. This bound for h_ϕ is found by solving the coexistence conditions at $\bar{n} = 1$, for $T = 0$. For increasing values of h_ϕ , the remaining triple point moves towards and eventually merges with the critical point of the quasi-binary region, leading to a coexistence region which has only one critical point (Fig. 2(c)). Finally, for larger values of h_ϕ , the system behaves as a binary mixture of charged macromolecules and solvent (Fig. 2(d)). In contrast, for $\lambda > 1/4$ and $h_\phi > h_{\phi,c}$, when the two regions merge, there is only one triple point, where two phases which are essentially enriched in charged macromolecules, coexist with a high concentration phase enriched in neutral macromolecules (Fig. 2(g)). For larger values of h_ϕ , the triple point vanishes together with the first order transition point at $T = 0$ and $\epsilon h_\phi = 2\chi(1/4 - \lambda)$. This

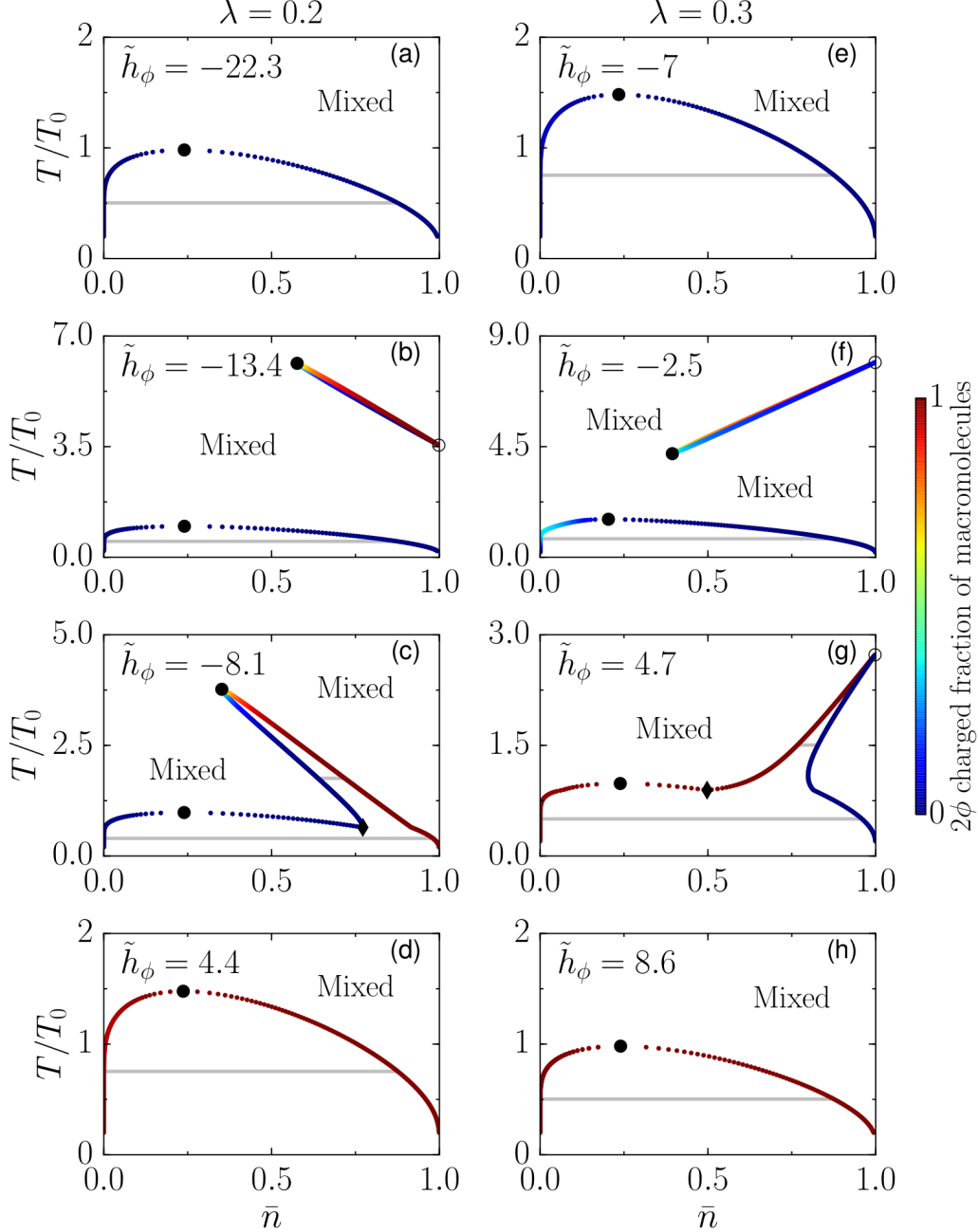


FIG. 2. Topologies of the phase diagrams for varying values of the normalized molecular field $\tilde{h}_\phi = h_\phi/k_B T_0$ defined in Eq. (27) where T_0 is a reference temperature. (a-d) phase diagrams for a system in which charge-charge interactions are slightly stronger than neutral-neutral interactions. (e-h) Phase diagrams for a system in which neutral-neutral interactions are slightly stronger than charge-charge interactions. The binodals are given by the coloured points which denote coexisting phases. Tie lines (grey solid lines) connect coexisting phases and are horizontal. The regions within the binodals undergo a demixing transition, whereas the regions outside the binodal lines remain well mixed. The critical points where phases become indistinguishable are denoted by black circles, first order transition points where there is a discontinuity in the value of ϕ are denoted by white circles and triple points are denoted by black diamonds. A thorough explanation of the phase diagrams is given in the main text. Parameters $\chi = -8.5$ and $\epsilon = 0.1$, apply to all panels. The colorbar indicates the value of the charged fraction of macromolecules ϕ .

vanishing leads again to the quasi-binary mixture of charged macromolecules and solvent (Fig. 2(h)).

The existence of a transition point on the $\bar{n} = 1$ line leads to the different topologies of the phase diagrams (Fig. 3). To understand the behaviour of this point, we analyse the derivative of the free energy density with respect to ϕ at $\bar{n} = 1$, in particular for $\lambda = 0.2$ (Fig. 3(a-c)). At the critical temperature, Eq. (36b), there is an inflection point (Fig. 3(a)), which translates into a critical point for $h_\phi = h_{\phi,c}$ at $T = T_c$ (Fig. 3(d)). For lower values of the temperature, $T < T_c$ one finds a first order transition point at $h_\phi > h_{\phi,c}$, in which two phases coexist at $\bar{n} = 1$ (Fig. 3(b,e)). For lower temperatures, the region which extends from the first order transition point merges with the rest of the phase diagram (Fig. 3(f)) and the derivative of the free energy density becomes increasingly dominated by a linear term in ϕ , given by $2\chi(\phi - \lambda)/\epsilon$ (Fig. 3(c)). For $T = 0$, there is a corresponding value of the molecular field, $\epsilon h_\phi = 2\chi(1/4 - \lambda)$, for which we find a solution to the coexistence conditions. For values $\epsilon h_\phi > 2\chi(1/4 - \lambda)$ there is no longer a transition point at $\bar{n} = 1$. We only focus on $\lambda = 0.2$ because the behaviour of the transition point at $\bar{n} = 1$ is similar for $\lambda > 0.25$. Now that we developed a detailed understanding of phase diagrams at the isoelectric point, we can use the developed framework to study the effects of varying pH.

VII. PHASE SEPARATION FOR VARYING PH

Here we study how deviations in pH with respect to the isoelectric point affect the phase behaviour of the system while keeping the temperature constant. To this end, we study phase diagrams as a function of pI – pH (Eq. (30)) and the total macromolecular volume fraction \bar{n} . We construct phase diagrams for different values of the molecular field h_ϕ , the interaction strength among charged macromolecules χ_e and the interaction strength among neutral macromolecules χ_n . Varying the pH in our model leads to very characteristic features in the phase diagrams which allow us to distinguish the dominant interaction driving phase separation.

Let us first consider the case where neutral molecules are energetically favoured over charged molecules ($h_\phi = -8$, Fig. 4(a-c)). In this case, a system with only charge-charge interactions (Fig. 4(a), $\chi_n = 0$) exhibits reentrant behaviour when changing the pH where the corresponding domain in the phase diagram is enclosed by two critical points. Beyond these points, phase separation is not possible for any value of the macromolecular volume fraction \bar{n} while between the critical points, there is a range in \bar{n} where phase separation can occur. The degree of such phase separation is maximal at the isoelectric point pH=pI, which is characterised by the largest difference between coexisting phases in their macromolecular volume fraction, as well as in their charged fraction between coexisting phases. Deviating from the isoelectric point corresponds to lowering the amount of one of the charged components ($\psi \neq 0$, Eq. (23)). This change in the relative composition between charged macromolecules decreases the interaction term among charged components (proportional to n_+n_-) and thereby lowers their propensity to phase separate. There is a small range in macromolecular volume fractions where phase separation is absent at the isoelectric point but can be triggered by changing the pH value away from pI. This range strongly increases for stronger interactions among neutral macromolecules (χ_n more negative, Fig. 4(b)). Such behaviour for phase separation is unexpected because phase separation occurs despite of an asymmetric ratio of the charged macromolecules. It emerges as a consequence of a reduction in the mixing entropy of the macromolecules by moving away from the isoelectric

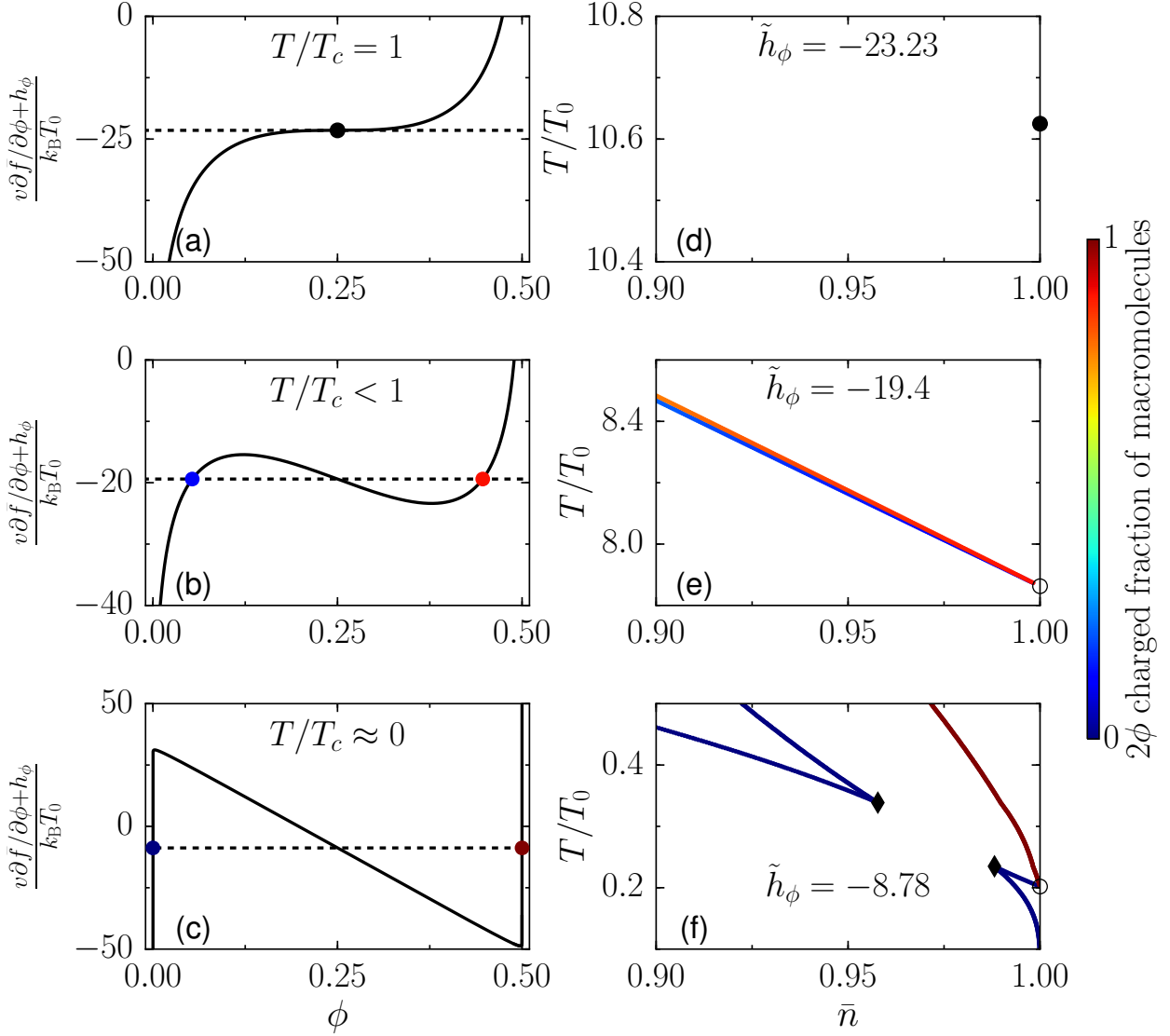


FIG. 3. Critical behaviour on the $\bar{n} = 1$ line. (a-c) Derivative of the free energy with respect to ϕ for different temperature values. (a) Inflection point corresponding to the critical point defined in Eq. (36) shown as a filled black circle. The black dotted line shows the value of $\tilde{h}_\phi = \tilde{h}_\phi^c \simeq -23.23$. (b) Emergence of a maximum and a minimum for $T < T_c$, coexisting phases are shown as two colored circles (the color encodes their value of ϕ). (c) Derivative of the free energy density for $T/T_0 = 0.2$, implying $T/T_c \ll 1$. (d-f) Phase diagrams for fixed $\tilde{h}_\phi = h_\phi/k_B T_0$ in the vicinity of the transition point at $\bar{n} = 1$. (d) The filled black circle is the isolated critical point defined in Eq. (36) corresponding to (a). (e) The phase coexistence lines shown in blue and red end on the $\bar{n} = 1$ line at the first order transition point (open circle) defined in (b). (f) The coexistence region connected to the $\bar{n} = 1$ axis, merges with the quasi-binary region, leading to the appearance of two triple points (black diamonds in (f)). Parameters $\chi = -8.5$, $\lambda = 0.2$ and $\epsilon = 0.1$, apply to all panels. T_0 is a reference temperature with $T_c/T_0 \simeq 10.6$.

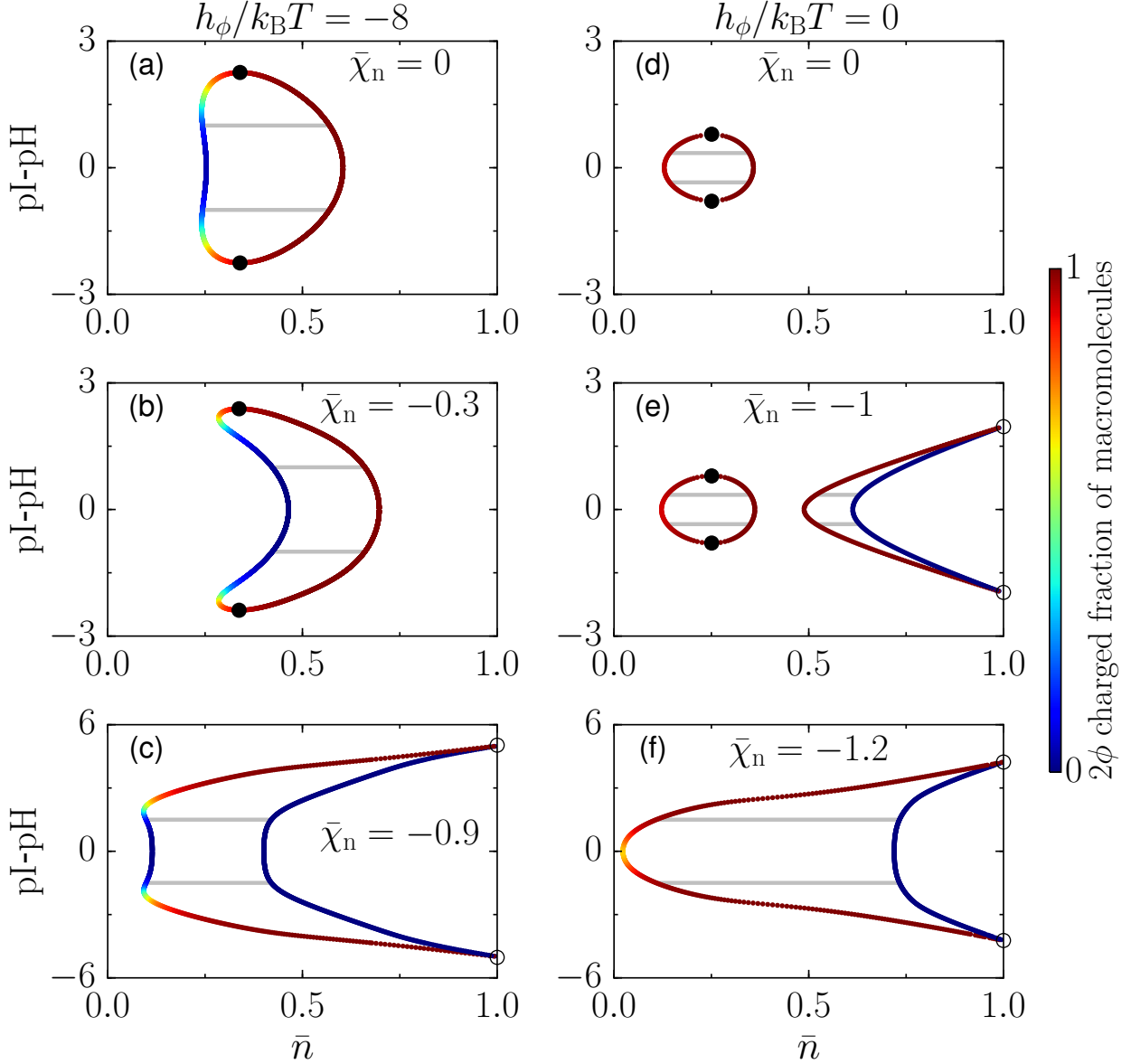


FIG. 4. Phase behaviour as a function of pH for fixed interaction strength between charges $\chi_e/k_B T = -3.5$ and varying values of the interaction strength $\bar{\chi}_n = \chi_n/k_B T$ between neutral macromolecules. (a-c) Phase diagrams with neutral macromolecules energetically favoured ($h_\phi/k_B T = -8$). (a) in the absence of neutral-neutral interactions there is a small region in the diagram where there is reentrant phase separation behaviour. (b) Small values of neutral-neutral interactions lead to a reduction of the demixing region. (c) Increasing the neutral-neutral attraction even further, the two critical points merge and two first order transition points appear at $\bar{n} = 1$, which has a discontinuity ϕ and ψ . (d-f) Phase diagrams with charged macromolecules energetically favoured ($h_\phi/k_B T = 0$): (d) An effective binary mixture at the pI shows a simple mixing behaviour while deviating from the isoelectric point. (e) For large enough interactions between neutral macromolecules, a second disconnected region appears, such region ends in two first order transition points at $\bar{n} = 1$. (f) Increasing the neutral-neutral interactions further, the two regions merge giving rise to a broadening of the demixing region while the critical points vanish and the coexistence region connects to the $\bar{n} = 1$ line with two first order transition points. Parameters $\epsilon = 0.1$ and $m = 1$ apply to all panels.

point which in turn allows the system to phase separate at lower values of charged fraction of macromolecules ϕ . Even though the system shows phase separation at lower macromolecular volume fraction, the region of phase separation decreases for increasing deviations from the isoelectric point. Increasing the attraction among neutral macromolecules even further leads to coexisting phases which are approximately composed of neutral macromolecules and solvent in a range of pH close to the isoelectric point (Fig. 4(c)). Moreover, two discontinuous phase transition points emerge while the two critical points merge and vanish. In contrast to the previous two cases (a,b) the broadest range in \bar{n} where phase separation occurs is not located at the isoelectric point (c). We must recognise that having such symmetric phase diagrams for pH deviations below and above the pI is a consequence of our choice of parameters, i.e. the charged macromolecules M^+ and M^- have equal molecular volumes and no interactions with the remaining components. Note that the internal free energies w_{M^+} and w_{M^-} only affect the value of the pI but not the symmetry of the phase diagrams around the pI.

We now discuss the effects of pH variations for a system in which charged macromolecules are energetically favoured over neutral ones. We start considering a mixture without neutral-neutral interactions (Fig. 4(d)) that exhibits a behaviour at the pI resembling a binary mixture of charged macromolecules and solvent (Fig. 2(d,f)). For values of pH away from the isoelectric point, we observe a monotonic decrease of the macromolecular order parameter, as well as a fairly constant charged fraction composition in both phases until they meet at two symmetric critical points. After switching on an attractive interaction among neutral macromolecules a second phase separation region appears at larger values of the total macromolecular volume fraction \bar{n} (Fig. 4(e)). This region is characterised by a high density phase mostly composed of neutral macromolecules coexisting with a phase rich in charged macromolecules. These two phases meet at two first order transition points (open symbol, Fig. 4(e)). The appearance of this region is a consequence of having an attraction among neutral macromolecules and charged macromolecules, respectively, favouring phase separation dominantly between both while the solvent is of rather similar concentration in the coexisting phases. Interestingly, the two regions behave independently from each other when increasing the attraction between macromolecules because each region is associated to a different solution of chemical equilibrium (Fig. 1(a)). While increasing the attraction further, the two regions merge (Fig. 4(f)). This merging leads to a broad region of phase separation corresponding to a large difference in the fraction of charged macromolecules and solvent as well as the vanishing of the two critical points. The high density phase is made of neutral macromolecules which coexist with a low density phase composed of solvent and charged macromolecules. We show the behaviour of ψ along the binodal lines in the same phase diagrams in the Supplementary Material.

One typical feature of most phase diagrams (Fig. 4(a,b,d-f)) is that the broader region of phase separation exists in the vicinity of the isoelectric point. The region of phase separation shrinks when deviating from the pI due to a decrease in interaction energy among charged macromolecules (Fig. 4(a,d)) or in the interaction energy among both charged macromolecules and neutral molecules (Fig. 4(b,e,f)). There is only clear exception among these phase diagrams (Fig. 4(c)), where the phase separation region slightly increases for pH values away from the isoelectric point. The increase is due to the emergence of another stable chemical branch which lowers the free energy by an increase in the mixing entropy in the low density phase and increasing the interaction among neutral macromolecules in the high density phase. One interesting feature of the phase diagrams, is that when the neutral-

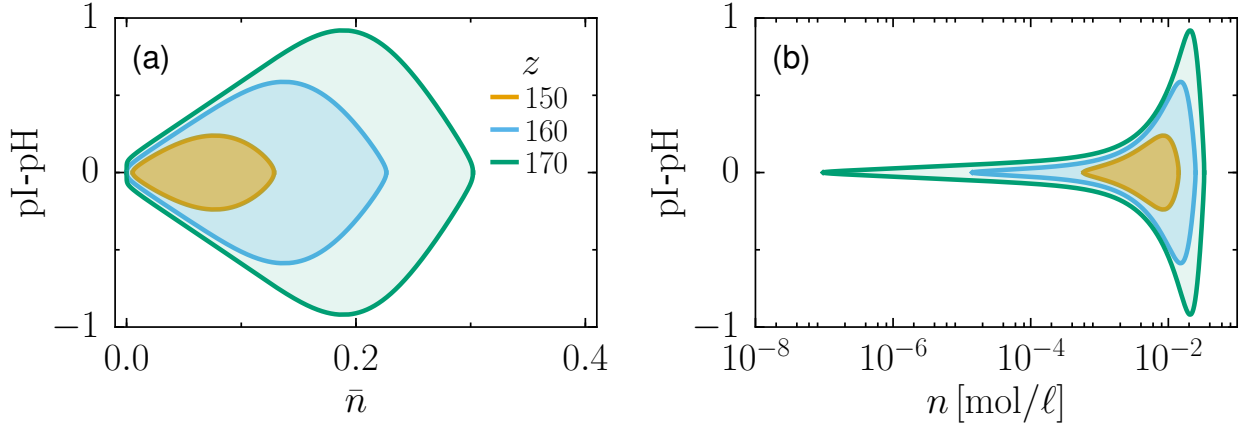


FIG. 5. Binodal lines for different choices of the total number of charges on the macromolecules z with interactions $\chi_e/k_B T = -\alpha z \epsilon$. The shaded region within the binodals is the region where macromolecules undergo a demixing transition, whereas the region outside is where the system remains homogeneously mixed. (a) Phase diagram as a function of the total macromolecule volume fraction \bar{n} and deviations from the isoelectric point $\text{pH} - \text{pI}$. (b) Same diagram as in (a) but as a function of the total macromolecule molar concentration n . Parameters $\epsilon = 0.002$, $h_\phi/k_B T = 10$ and $\alpha = 7.5$, apply to both panels.

neutral interactions become dominant, i.e., the phase behavior at the isoelectric point is mainly driven by the interaction among neutral macromolecules, we observe the vanishing of the critical points, giving rise to phase diagrams which only have first order transitions. The dominant interaction thus defines the topology of the phase diagram as a function of pH.

Finally, we study a more realistic scenario where the maximal net charge of the macromolecules m is chosen to be $m = 50$, which is close to the net maximal charge of some proteins that respond to pH changes and that are found in the so called stress granules [9, 24, 25]. For simplicity we only consider interactions between oppositely charged macromolecules, which in this case are given by $\chi_e/\epsilon = -\alpha z k_B T$, where z is the total number of charges of the macromolecule and α is a factor describing the contribution of each fixed charge of the macromolecules to the interaction (we use the value $\alpha = 7.5$ as reported in [26]). We study the system for three different values of the total number of charges in the macromolecule z and choosing $\epsilon = 0.002$ (Fig. 5) motivated by a volume ratio of water molecules and a typical protein. For all values of z considered, there exists a broad region of phase separation at the isoelectric point (Fig. 5). The coexistence becomes broader for increasing values of z due to an increase in the interaction strength. Our minimal model predicts that at the isoelectric point, a mixture of macromolecules with a large total number of charges, will phase separate over a large concentration range. Finally, we also show that reducing z can lead to a drastic reduction of the concentration range in which the system undergoes phase separation (Fig. 5(b)).

VIII. DISCUSSION

In this manuscript, we have established a thermodynamic framework to study liquid-liquid phase separation in a system where the pH is controlled. We started by introducing chemical reactions controlling the charge states of macromolecules which are in turn determined by the pH value of the mixture. Using conservation laws for a system undergoing chemical reactions, we identified the effective thermodynamic conjugate variables at chemical equilibrium. We then found the relevant thermodynamic variables controlling the pH of the system, namely the chemical potential difference $\mu_{\text{H}_3\text{O}^+} - \mu_{\text{H}_2\text{O}}$ and the temperature T . That allowed us to construct the corresponding thermodynamic potentials for a system with a fixed pH value by means of a Legendre transform which makes $\mu_{\text{H}_3\text{O}^+} - \mu_{\text{H}_2\text{O}}$ a natural variable of the corresponding free energy. Based on these thermodynamic potentials we showed how the chemical and phase equilibrium are controlled by the pH of the system and calculated the corresponding phase diagrams.

We found that phase separation typically occurs around pH values corresponding to the isoelectric point pI. Our results could be relevant to cell behavior, where there is a protein spectrum, in which many cytosolic proteins have isoelectric points around pH = 5. These results are consistent with observations in yeast cells [12] where many proteins separate from the cytosol once the pH is lowered to pH=5. Using typical parameters for cellular proteins (Fig. 5) we find that phase separation occurs from concentrations ranging from μM corresponding to a typical saturation concentration of phase separating cellular proteins [9, 11] to mM. Our model is also in agreement with phase separation for a concentration of the order of 1 mM, which is an estimation of the total concentration of proteins in yeast [27]. Note that phase separation is lost both at low and high concentrations, which can be understood from the analogy with the quasi-binary mixture shown in Fig. (2)(a,e). We further predict that upon decreasing pH even more, reentrant behaviour leading to a mixed state will be observed. However, this behaviour may not always be observable in living systems due to several reasons. One of them is that upon decreasing the pH below the isoelectric point, proteins might denature and aggregate irreversibly before reaching conditions for phase separation that we describe in this manuscript. Our approach considers phase separation controlled by pH at thermodynamic equilibrium. Neglecting the effect on phase separation related to the consumption of ATP is reasonable since the reported starvation induced phase separation occurs upon ATP depletion conditions [12]. In the future we will consider to extend our approach to out of equilibrium situations.

ACKNOWLEDGMENTS

V.Z. acknowledges financial support from Volkswagen Foundation “Life?” initiative.

REFERENCES

- [1] B. Alberts, *Molecular biology of the cell* (Garland science, New York, 2017).
- [2] C. P. Brangwynne, C. R. Eckmann, D. S. Courson, A. Rybarska, C. Hoege, J. Gharakhani, F. Jülicher, and A. A. Hyman, *Science* **324**, 1729 (2009).
- [3] A. Molliex, J. Temirov, J. Lee, M. Coughlin, A. Kanagaraj, H. Kim, T. Mittag, and J. Taylor, *Cell* **163**, 123 (2015).
- [4] D. Zwicker, M. Decker, S. Jaensch, A. A. Hyman, and F. Jülicher, *Proceedings of the National Academy of Sciences* **111**, E2636 (2014).
- [5] C. P. Brangwynne, *The Journal of Cell Biology* **203**, 875 (2013).
- [6] S. Elbaum-Garfinkle, Y. Kim, K. Szczepaniak, C. C.-H. Chen, C. R. Eckmann, S. Myong, and C. P. Brangwynne, *Proceedings of the National Academy of Sciences* **112**, 7189 (2015).
- [7] L. Zhu and C. P. Brangwynne, *Current Opinion in Cell Biology* **34**, 23 (2015), cell nucleus.
- [8] S. F. Banani, H. O. Lee, A. A. Hyman, and M. K. Rosen, *Nature reviews Molecular cell biology* **18**, 285 (2017).
- [9] T. M. Franzmann, M. Jahnel, A. Pozniakovsky, J. Mahamid, A. S. Holehouse, E. Nüske, D. Richter, W. Baumeister, S. W. Grill, R. V. Pappu, A. A. Hyman, and S. Alberti, *Science* **359**, eaao5654 (2018).
- [10] A. Patel, H. O. Lee, L. Jawerth, S. Maharana, M. Jahnel, M. Y. Hein, S. Stoyanov, J. Mahamid, S. Saha, T. M. Franzmann, A. Pozniakovski, I. Poser, N. Maghelli, L. A. Royer, M. Weigert, E. W. Myers, S. Grill, D. Drechsel, A. A. Hyman, and S. Alberti, *Cell* **162**, 1066 (2015).
- [11] S. Saha, C. A. Weber, M. Nusch, O. Adame-Arana, C. Hoege, M. Y. Hein, E. Osborne-Nishimura, J. Mahamid, M. Jahnel, L. Jawerth, , A. Pozniakovski, C. R. Eckmann, F. Jülicher, and A. A. Hyman, *Cell* **166**, 1572 (2016).
- [12] M. C. Munder, D. Midtvedt, T. Franzmann, E. Nuske, O. Otto, M. Herbig, E. Ulbricht, P. Mller, A. Taubenberger, S. Maharana, L. Malinowska, D. Richter, J. Guck, V. Zaburdaev, and S. Alberti, *eLife* **5**, e09347 (2016).
- [13] R. A. Alberty, *Chemical reviews* **94**, 1457 (1994).
- [14] R. Buck, S. Rondinini, A. Covington, F. Baucke, C. Brett, M. Camões, M. Milton, T. Mussini, R. Naumann, K. Pratt, R. Spitzer, and G. Wilson, *Pure and Applied Chemistry* **74**, 2169 (2002).
- [15] I. Mills, T. Cvitaš, K. Homann, N. Kallay, and K. Kuchitsu, *Quantities, Units and Symbols in Physical Chemistry* (Blackwell Science, Oxford, 1993).
- [16] D. Marx, M. E. Tuckerman, J. Hutter, and M. Parrinello, *Nature* **397**, 601 (1999).
- [17] J. M. Headrick, E. G. Diken, R. S. Walters, N. I. Hammer, R. A. Christie, J. Cui, E. M. Myshakin, M. A. Duncan, M. A. Johnson, and K. D. Jordan, *Science* **308**, 1765 (2005).
- [18] M. L. Huggins, *The Journal of Physical Chemistry* **9**, 441 (1941).
- [19] P. J. Flory, *The Journal of Chemical Physics* **10**, 51 (1942).
- [20] H. B. Callen, *Thermodynamics and an introduction to thermostatistics* (John Wiley and Sons, New York, 1985).
- [21] R. Scheu, B. M. Rankin, Y. Chen, K. C. Jena, D. Ben-Amotz, and S. Roke, *Angewandte Chemie International Edition* **53**, 9560 (2014).
- [22] S. A. Safran, *Statistical thermodynamics of surfaces, interfaces, and membranes* (Addison-Wesley, Reading, 1994).
- [23] M. Rubinstein and R. H. Colby, *Polymer physics* (Oxford University Press, Oxford, 2003).

- [24] J. A. Riback, C. D. Katanski, J. L. Kear-Scott, E. V. Pilipenko, A. E. Rojek, T. R. Sosnick, and D. A. Drummond, [Cell](#) **168**, 1028 (2017).
- [25] The proteins Sup35 and Pab1, which respond to pH changes have net charges within this range and the total number of charges is approximately as high as 184 for Sup35.
- [26] D. Harries, S. May, and A. Ben-Shaul, [Soft Matter](#) **9**, 9268 (2013).
- [27] R. Milo, [BioEssays](#) **35**, 1050 (2013).

SUPPLEMENTARY MATERIAL

1. pH in diluted systems

We now show that our definition of pH given in Eq. (15)) is equivalent to the most commonly used definition $\text{pH} = -\log_{10}(n_{\text{H}_3\text{O}^+}/n_{\text{H}_3\text{O}^+}^0)$, which only applies for ideal solutions of H_3O^+ and OH^- in water. In the absence of macromolecules and considering ideal solution conditions, the chemical potentials of water $\mu_{\text{H}_2\text{O}}$ and of hydronium ions $\mu_{\text{H}_3\text{O}^+}$ can be expressed as

$$\mu_{\text{H}_2\text{O}} = v_0 P + w_{\text{H}_2\text{O}} \quad , \quad (\text{S.1})$$

$$\mu_{\text{H}_3\text{O}^+} = k_{\text{B}} T \ln(v_0 n_{\text{H}_3\text{O}^+}) + v_{\text{H}_3\text{O}^+} P + w_{\text{H}_3\text{O}^+} \quad , \quad (\text{S.2})$$

where we assumed that the contribution of the ions to the volume V is negligible, i.e. taking the volume fraction of water $v_0 n_{\text{H}_2\text{O}} = 1$. The standard chemical potentials $\mu_{\text{H}_2\text{O}}^0$ and $\mu_{\text{H}_3\text{O}^+}^0$ are given by the following expressions

$$\mu_{\text{H}_2\text{O}}^0 = v_0 P + w_{\text{H}_2\text{O}} \quad , \quad (\text{S.3})$$

$$\mu_{\text{H}_3\text{O}^+}^0 = k_{\text{B}} T \ln(v_0 n_{\text{H}_3\text{O}^+}^0) + v_{\text{H}_3\text{O}^+} P + w_{\text{H}_3\text{O}^+} \quad . \quad (\text{S.4})$$

Substituting Eqs. (S.1)-(S.4) in the definition given in Eq. (15) we obtain

$$\text{pH} = -\log_{10} \left(\frac{n_{\text{H}_3\text{O}^+}}{n_{\text{H}_3\text{O}^+}^0} \right) \quad . \quad (\text{S.5})$$

2. Chemical potentials

Here we write the explicit form of the chemical potentials, which are given by

$$\mu_{\text{M}} = k_{\text{B}} T (\ln(v n_{\text{M}}) + 1) + 2 \frac{v}{\epsilon} \chi_{\text{n}} n_{\text{M}} + w_{\text{M}} + v(P - \Sigma) \quad , \quad (\text{S.6a})$$

$$\mu_{\text{M}^+} = k_{\text{B}} T (\ln(v n_{\text{M}^+}) + 1) + \frac{v}{\epsilon} \chi_{\text{e}} n_{\text{M}^-} + w_{\text{M}^+} + v(P - \Sigma) \quad , \quad (\text{S.6b})$$

$$\mu_{\text{M}^-} = k_{\text{B}} T (\ln(v n_{\text{M}^-}) + 1) + \frac{v}{\epsilon} \chi_{\text{e}} n_{\text{M}^+} + w_{\text{M}^-} + v(P - \Sigma) \quad , \quad (\text{S.6c})$$

$$\mu_{\text{H}_3\text{O}^+} = k_{\text{B}} T (\ln(v_0 n_{\text{H}_3\text{O}^+}) + 1) + w_{\text{H}_3\text{O}^+} + v_0(P - \Sigma) \quad , \quad (\text{S.6d})$$

$$\mu_{\text{OH}^-} = k_{\text{B}} T (\ln(v_0 n_{\text{OH}^-}) + 1) + w_{\text{OH}^-} + v_0(P - \Sigma) \quad , \quad (\text{S.6e})$$

$$\mu_{\text{H}_2\text{O}} = k_{\text{B}} T (\ln(v_0 n_{\text{H}_2\text{O}}) + 1) + w_{\text{H}_2\text{O}} + v_0(P - \Sigma) \quad . \quad (\text{S.6f})$$

3. Choice of conserved quantities

From the reaction scheme (1) we identify three conserved components in every chemical reaction, which are

$$N = N_{M^+} + N_{M^-} + N_M \quad , \quad (\text{S.7})$$

$$N_H = 3N_{\text{H}_3\text{O}^+} + m(2N_{M^+} + N_M) + N_{\text{OH}^-} + 2N_{\text{H}_2\text{O}} \quad , \quad (\text{S.8})$$

$$N_s = N_{\text{H}_3\text{O}^+} + N_{\text{OH}^-} + N_{\text{H}_2\text{O}} \quad , \quad (\text{S.9})$$

the three conserved components are: N the total number of macromolecules, N_H the number of hydrogen atoms and N_s is the number of oxygen atoms. We can combine these equations to show that the partial charge involved in the chemical reactions $N_q = N_H - 2N_s - mN$ is also a constant given by

$$N_q = N_{\text{H}_3\text{O}^+} + m(N_{M^+} - N_{M^-}) - N_{\text{OH}^-} \quad . \quad (\text{S.10})$$

4. Concentration of water and its ions at chemical equilibrium

Using Eq. (24c) and the chemical potential difference $\mu_{\text{H}_3\text{O}^+} - \mu_{\text{H}_2\text{O}}$, we introduce two more fields controlling the relative concentrations of hydronium and hydroxide ions with respect to water molecules, these fields obey

$$\log\left(\frac{n_{\text{H}_3\text{O}^+}}{n_{\text{H}_2\text{O}}}\right) = \frac{h_H}{k_B T} + \frac{h_\psi}{2mk_B T} \quad , \quad (\text{S.11})$$

$$\log\left(\frac{n_{\text{OH}^-}}{n_{\text{H}_2\text{O}}}\right) = \frac{h_O}{k_B T} - \frac{h_\psi}{2mk_B T} \quad , \quad (\text{S.12})$$

where the fields h_H and h_O are defined by

$$h_H = \frac{w_{M^+} - w_{M^-}}{2m} - w_{\text{H}_3\text{O}^+} + w_{\text{H}_2\text{O}} \quad , \quad (\text{S.13})$$

$$h_O = \frac{w_{M^-} - w_{M^+}}{2m} - w_{\text{OH}^-} + w_{\text{H}_2\text{O}} \quad . \quad (\text{S.14})$$

We can go further and use the condition $v_0 n_s + v n = 1$ and Eqs. (S.11) and (S.12) to express the concentrations of hydronium ions, hydroxide ions and water molecules as a function of the total macromolecule density n , temperature T and pH (or h_ψ), given by

$$n_{\text{H}_2\text{O}} = \frac{1 - v n}{v_0 \left(1 + e^{h_H/k_B T + h_\psi/2mk_B T} + e^{h_O/k_B T - h_\psi/2mk_B T}\right)} \quad , \quad (\text{S.15})$$

$$n_{\text{H}_3\text{O}^+} = \frac{(1 - v n) e^{h_H/k_B T + h_\psi/2mk_B T}}{v_0 \left(1 + e^{h_H/k_B T + h_\psi/2mk_B T} + e^{h_O/k_B T - h_\psi/2mk_B T}\right)} \quad , \quad (\text{S.16})$$

$$n_{\text{OH}^-} = \frac{(1 - v n) e^{h_O/k_B T - h_\psi/2mk_B T}}{v_0 \left(1 + e^{h_H/k_B T + h_\psi/2mk_B T} + e^{h_O/k_B T - h_\psi/2mk_B T}\right)} \quad . \quad (\text{S.17})$$

5. Critical points at the isoelectric point

In this section we calculate some limiting critical values at the isoelectric point, where $\psi = 0$ and $h_\psi = 0$.

a. Effective binary critical point

In order to calculate the critical points describing the effective binary mixture, we first discuss the limits of h_ϕ for $\phi \rightarrow 1/2$ and $\phi \rightarrow 0$, which correspond to situations where macromolecules are only charged or only neutral respectively.

If we consider the limit of h_ϕ with $\phi \rightarrow 1/2$,

$$\begin{aligned} \lim_{\phi \rightarrow \frac{1}{2}} h_\phi &= \lim_{\phi \rightarrow \frac{1}{2}} \left[2k_B T \ln \frac{\phi}{1-2\phi} + \chi \bar{n} (\phi - \lambda) / \epsilon \right] , \\ \lim_{\phi \rightarrow \frac{1}{2}} h_\phi &= -2 \ln 2 - 2k_B T \lim_{\phi \rightarrow \frac{1}{2}} \ln(1-2\phi) + \frac{\chi \bar{n}}{\epsilon} \left(\frac{1}{2} - \lambda \right) , \\ \lim_{\phi \rightarrow \frac{1}{2}} h_\phi &= \infty , \end{aligned}$$

this shows on one hand that large positive values of h_ϕ are obtained for values of ϕ approaching $1/2$, on the other hand, large negative values of h_ϕ are obtained for ϕ approaching 0.

$$\lim_{\phi \rightarrow 0} h_\phi = -\infty .$$

We can study both cases by direct substitution in the free energy density (31). We illustrate the case for $\phi = 1/2$, in this case the free energy density reads:

$$v \bar{f} = k_B T \left(\bar{n} \ln \left(\frac{\bar{n}}{2} \right) + \frac{(1-\bar{n})}{\epsilon} \ln(1-\bar{n}) \right) + \frac{\chi_e \bar{n}^2}{4\epsilon} + \mathcal{O}(\bar{n}) , \quad (\text{S.18})$$

the linear terms $\mathcal{O}(\bar{n})$ do not affect the stability of the system, therefore we are safe to ignore them in our calculation. From the free energy evaluated at $\phi = 1/2$ (S.18), we calculate the chemical potential up to a constant

$$v \frac{d\bar{f}}{d\bar{n}} = k_B T \left[\ln \left(\frac{\bar{n}}{2} \right) + 1 - \frac{\ln(1-\bar{n}) + 1}{\epsilon} + \frac{\chi_e \bar{n}}{2\epsilon} \right] \quad (\text{S.19})$$

using Eq. (S.19) and conditions $d^2 f / d\bar{n}^2 = 0$ and $d^3 f / d\bar{n}^3 = 0$ we find

$$\bar{n}_c^b = \frac{\sqrt{\epsilon}}{1 + \sqrt{\epsilon}} , \quad (\text{S.20})$$

$$k_B T_c = -\frac{\chi_e}{2(1 + \sqrt{\epsilon})^2} . \quad (\text{S.21})$$

Following the same procedure for a system with $\phi = 0$ gives

$$\bar{n}_c^b = \frac{\sqrt{\epsilon}}{1 + \sqrt{\epsilon}} , \quad (\text{S.22})$$

$$k_B T_c = -2 \frac{\chi_n}{(1 + \sqrt{\epsilon})^2} . \quad (\text{S.23})$$

b. *Critical point at $\bar{n} = 1$*

Here, we calculate the critical value which emerges at $\bar{n} = 1$ using the free energy density (31), which at the isoelectric point is

$$v\bar{f} = k_{\text{B}}T(2\phi \ln \phi + (1 - 2\phi) \ln(1 - 2\phi)) + \chi(\phi^2 - 2\lambda\phi + \lambda/2)/\epsilon - h_{\phi}\phi + w_{\text{M}} \quad (\text{S.24})$$

We first differentiate \bar{f} with respect to ϕ which gives

$$v\frac{\partial \bar{f}}{\partial \phi} = k_{\text{B}}T(2 \ln \phi - 2 \ln(1 - 2\phi)) + 2\chi(\phi - \lambda)/\epsilon - h_{\phi} \quad . \quad (\text{S.25})$$

The conditions for finding a critical point in this case are $\partial^2 \bar{f}/\partial \phi^2 = 0$ and $\partial^3 \bar{f}/\partial \phi^3 = 0$, these conditions read

$$k_{\text{B}}T_c \left(\frac{2}{\phi_c} + \frac{4}{1 - 2\phi_c} \right) + 2\chi/\epsilon = 0 \quad , \quad (\text{S.26})$$

$$k_{\text{B}}T_c \left(-\frac{2}{\phi_c^2} + \frac{8}{(1 - 2\phi_c)^2} \right) = 0 \quad . \quad (\text{S.27})$$

Solving Eqs. (S.26) and (S.27) we find

$$\phi_c = \frac{1}{4} \quad , \quad (\text{S.28})$$

$$k_{\text{B}}T_c = -\frac{\chi}{8\epsilon} \quad , \quad (\text{S.29})$$

$$h_{\phi,c} = \chi \left(\frac{\ln 2 + 2 - 8\lambda}{4\epsilon} \right) \quad . \quad (\text{S.30})$$

6. Phase diagrams as a function of pH

Here we show the phase diagrams from Fig. 4 showing the dependence in ψ .

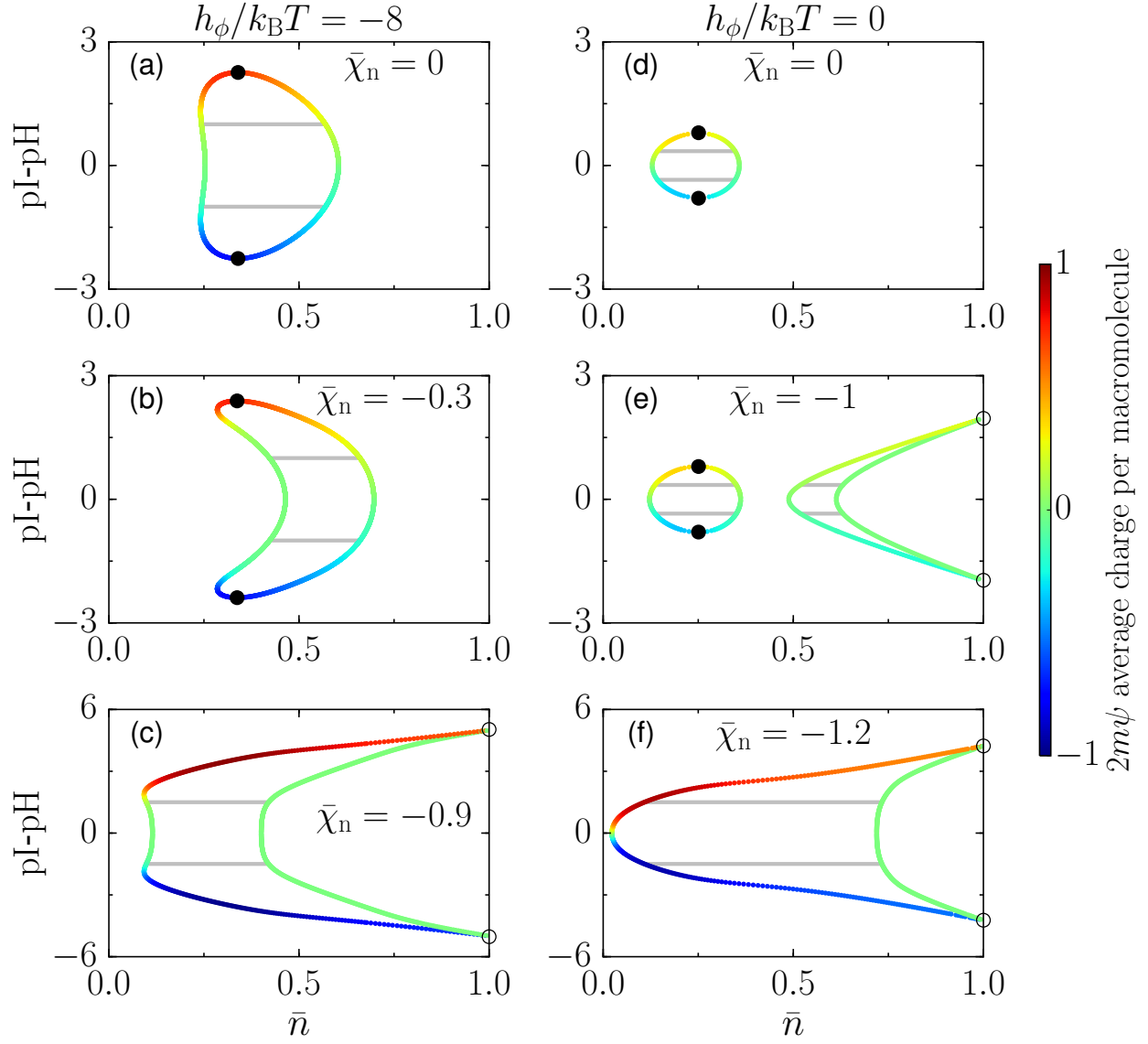


FIG. 6. Phase behaviour as a function of pH, the colorbar indicates the average charge per macromolecule $2m\psi = m(n_{M^+} - n_{M^-})/n$. Parameters $\epsilon = 0.1$ and $\chi_e/k_B T = -3.5$, apply to all panels.